SSC09-XI-9

Peak Power Tracking on a Nanosatellite Scale: The Design and Implementation of Digital Power Electronics on the SFL Generic Nanosatellite Bus

Grant Bonin[1], Doug Sinclair[2], and Robert E. Zee[1]

[1]UTIAS Space Flight Laboratory
4925 Dufferin St., Toronto, ON. Canada M3H 5T6; +1-416-667-7993
gbonin@utias-sfl.net; rzee@utias-sfl.net

[2]Sinclair Interplanetary
268 Claremont St., Toronto, ON. Canada M6J 2N3; +1-647-286-3761
dns@sinclairinterplanetary.com

ABSTRACT

This paper describes the design and implementation of an advanced high-performance nanosatellite power system, with an emphasis on its battery management and peak power tracking (PPT) capabilities. This power system has been developed for the University of Toronto Institute for Aerospace Studies' Space Flight Laboratory (UTIAS/SFL) Generic Nanosatellite Bus (GNB), which has enabled a wide variety of new space applications on a small scale. The GNB has a 20cm cubical form factor with no deployed solar arrays, making it inherently power-limited. Consequently, the need to accommodate relatively high powered payloads for multi-year missions has dictated the need for maximum utilization of solar power, and with maximum efficiency. To accomplish this, the GNB power system implements an unconventional parallel-regulated Direct Energy Transfer (DET) architecture with PPT functionality using a single bi-directional digital switch-mode power converter per battery, which also permits multiple redundant batteries as required. The trade space between different power system architectures is explored for missions of this class, and a parallel-regulated DET bus is shown to be the regulated topology of highest efficiency, advantageous when the range of solar array and bus voltages for a spacecraft are closely matched. The primary regulation device—referred to as a Battery Charge/Discharge Regulator (BCDR)—is described, and the advantages of its design are discussed. Finally, a new variant on conventional peak power tracking—referred to as *Peak Current Tracking* (PCT)—is discussed. The PCT algorithm is implemented using spacecraft BCDRs, and works to maximize battery charge current as well as to minimize battery discharge current. PCT operates during both sunlight and eclipse, and interrogates the entire system to determine the optimal voltage for battery charge management, which is an emergent property of the technique. PCT is shown to reduce battery depth-of-discharge by almost 20% compared to systems with fixed system voltages. The GNB power system design represents a significant advance over what has previously been implemented on a nanospacecraft scale, further enabling advanced missions on a power-limited platform.

INTRODUCTION

As the capabilities of microspacecraft and nanospacecraft continue to increase, it has become generally accepted that smaller satellites can offer substantially reduced-cost approaches to an ever growing variety of space missions [1]. The University of Toronto Institute for Aerospace Studies' Space Flight Laboratory (UTIAS/SFL) undertakes advanced small spacecraft research and development in order to leverage and expand such capabilities, assisting scientific, commercial and military organizations worldwide in realizing valuable space objectives. Small spacecraft are envisioned by some [2] as a powerful technical and economic mechanism for increasing the frequency and cost-effectiveness of space missions in general.

The Generic Nanosatellite Bus (GNB)

As the number and scope of SFL nanosatellite missions have increased, the need for an advanced, quickly reconfigurable bus design has arisen [3]. In order to address this need, UTIAS/SFL has developed a Generic Nanosatellite Bus (GNB) design capable of accommodating a wide variety of payloads. GNB (Figure 1) is a 20cm cubical spacecraft design massing less than 10 kg, with an approximately 17 x 13 x 8 cm internal payload volume. This central payload volume sits between two trays which house the majority of spacecraft

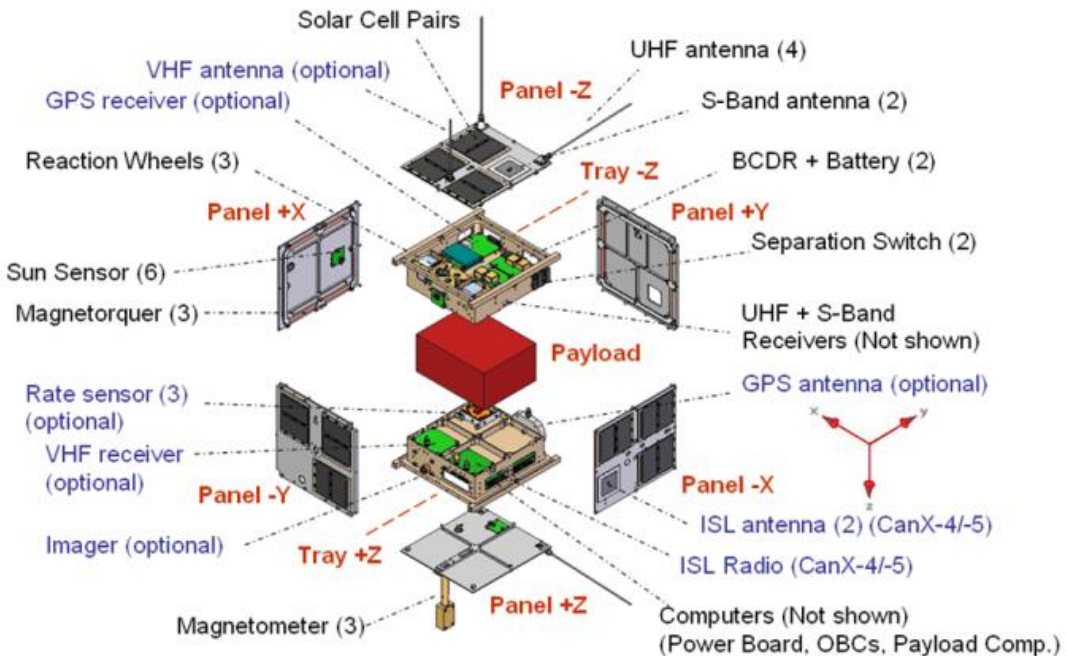

Figure 1: The Generic Nanosatellite Bus [4]

electronics and actuators. These trays connect together via payload mounting brackets and external panels, which also serve as mounting surfaces for solar cells and antennas.

The Generic Nanosatellite Bus has solar arrays on all panels, each of which nominally generates approximately 5.7W under worst-case-hot end-of-life (WCH/EOL) conditions. The GNB power system is additionally capable of regulating the system operating voltage such that maximum power can be extracted from solar panels as required. GNB incorporates a full-duplex communication system comprised of a 4 kbps UHF receiver and a 32 kbps S-Band transmitter, with an antenna complement consisting of four UHF quad-canted monopole and two S-Band patch antennas, each of which provides near-omnidirectional coverage. Each GNB spacecraft is three-axis stabilized, using three reaction wheels for precision attitude control and three magnetorquers for coarse control and momentum dumping. The default equipment complement of GNB additionally consists of three on-board computers (OBCs), each identical in design and connected in parallel for redundancy; a precision magnetometer, six fine sun sensors, and three orthogonal rate sensors for attitude determination; a single-band GPS receiver; two batteries and accompanying BCDRs; and one central power board for separation switches, load power switches, and regulated voltage supplies.

GNB is highly reconfigurable. Any of the equipment described above can be omitted (or in some cases, additional units included) as required. The operational orbit for GNB missions is nominally 500 to 700 km sun-synchronous, and as part of the GNB philosophy, the thermo-optical properties of all GNB spacecraft can be tailored to achieve passive thermal control for any Local Time of Ascending Node (LTAN). Finally, the GNB structure includes four launch rails to allow spacecraft deployment from the UTIAS/SFL eXperimental Push-Out Deployer (XPOD) deployment system, which—like GNB—is designed to be readily adapted to ejecting a number of different spacecraft designs from a wide variety of launch vehicles.

Current GNB missions include:

- AISSat-1 (maritime monitoring using automatic identification system signals);
- UniBRITE and BRITE-Austria (stellar astronomy); and
- CanX-4/-5 (Formation flight demonstration)

AISSat-1 is scheduled to launch in the fall of 2009, with BRITE and CanX-4/-5 spacecraft slated for launch in 2010. Additional missions and growth concepts are also being developed at SFL.

BACKGROUND

Peak Power Tracking on Small Spacecraft

The utility of small spacecraft is greatly limited by their ability to generate power; and as the broad trend towards reduced bus size and increased mission life continues, there will be growing pressure on small satellite

platforms to both produce more power and to utilize power more efficiently.

Tracking the maximum power point of a photovoltaic (PV) system has become an essential part of PV systems in terrestrial applications [5], as well as on low-Earth orbit microsatellites. However, the benefits of peak power tracking are not yet widely taken advantage of by nano- and picospacecraft [6]. Instead, it is frequently the case that very small spacecraft PV systems dramatically under-utilize the power-generating capability of their solar panels, in principle on the basis of reducing system mass and complexity [6].

In the canonical small spacecraft direct energy transfer bus, solar arrays are either clamped at the battery voltage or shunt-regulated to a desired operating point. No switch-mode converters are required in this sort of design, and consequently, parts count and mass are reduced and efficiency in the forward power path is increased. However, while such designs benefit spacecraft with large solar arrays in high orbits (where power generation is relatively cheap and array temperatures change less dramatically), for small spacecraft in low-Earth orbits, the archetypal DET system is a false economy [6]. In [6], Clark observes that, in the LEO environment, a DET bus is only able to generate maximum solar power when its battery voltage is near the solar array peak power point and solar panels are hot—that is, when the battery is fully charged and solar panels are at their lowest performance. Under these circumstances, excess power available from the array must be shunted to avoid over-charging spacecraft batteries. Put another way: the DET system in LEO provides maximum power only when it's needed least.

Conversely, the use of peak power tracking offers the prospect of maximum solar array utilization throughout the entire sunlit period of each orbit. This is particularly useful immediately after eclipse, when spacecraft batteries are most discharged and solar arrays can produce the most power. A PPT bus allows the spacecraft to take in the exact amount of power it requires for loads and battery charging, up to the maximum power point of solar arrays; and consequently, the full capabilities of the PV system can be leveraged throughout the entire mission life, and across the full range of array temperature variations. These two factors are strong motivation for PPT use on power-limited platforms.

The GNB power system can leverage the benefits of peak power tracking to an even greater extent than conventional missions by employing a novel technique, referred to here as *Peak Current Tracking* (PCT). PCT is predicated on maximizing *battery charge current* instead of solar array power, allowing the battery to charge as quickly as possible under both linear and constant power loads. Furthermore, the process of maximizing battery charge current also *minimizes battery discharge*, which provides the added benefit of reducing battery discharge in eclipse. Whereas the canonical peak power tracking system interrogates the spacecraft solar array to find a setpoint for maximum power output (which is usually but not always best for charging batteries), the PCT approach interrogates the entire system in order to find the optimal voltage for battery charge management, during both sunlight and eclipse. This approach, implemented using a simple, robust and modular topology, represents an important advance in the field of small spacecraft power system design.

THE GNB POWER SYSTEM

Overview

The GNB power system is a unique PV-battery architecture that implements a fully-regulated direct energy transfer bus with peak power tracking functionality, [8]. In this architecture, a single parallel battery charge/discharge regulator (BCDR) is used to set the operating voltage of the solar array and bus, regulate battery current, and monitor telemetry, including voltage, current and temperature. Power switches and regulated voltage supplies are located on a central power board with a firmware power controller implemented on a single programmable logic device (PLD) used to control all switched loads. The power controller is responsible for decoding all switch states and telemetry commands issued by either of two identical on-board computers (OBCs). Hardware overcurrent protection is used on all switches to prevent bus voltage decay in the event of load faults. Software overcurrent monitoring and protection is also implemented for all resettable (latching) switches. Point-of-load voltage regulation is performed by most subsystems, with regulated 3V, 5V, and either 3.3V or 10V rails provided by the power board as required. 12-bit analog-to-digital converters (ADC) on the power board collect telemetry from various sensors, including current and temperature from each solar panel; bus and battery voltage; load currents; and main switch current. A 12-bit digital-to-analog converter (DAC) drives programmable constant current sources for three spacecraft magnetorquers. A simple illustration of the GNB power system is presented in Figure 2.

Power Generation

The GNB design uses triple-junction $InGaP_2$/GaAs/Ge solar cells which have a nominal power conversion efficiency of 26.8% at beginning of life (BOL). Each individual solar cell is capable of generating approximately 1W at its maximum power point. All solar cells

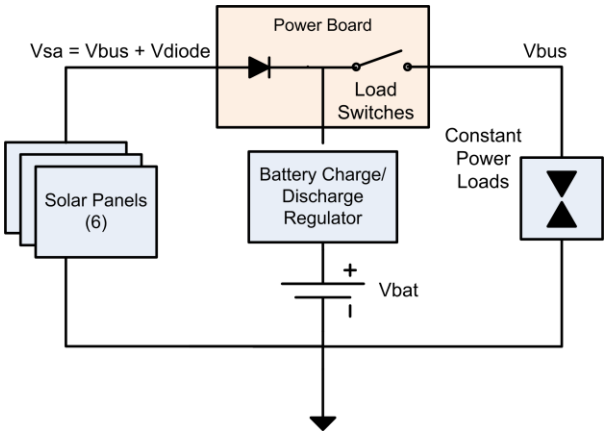

Figure 2: Simplified GNB Power System Topology

are protected physically by a layer of coverglass and electrically by an integral bypass diode.

The power board used on GNB allows connection of up to 22 solar power inputs to the bus. Each solar panel on GNB consists of the cells from one spacecraft face. Cells are series-connected in pairs, with every cell pair connected in parallel via the power board. This configuration was chosen to give cell pair operating voltages close to the battery, with a maximum solar panel range of $3.5V < V_{sa} < 5.5V$. Each solar panel connects to the power board via a single connector. The wiring harness consists of 24 AWG Teflon-coated wire with one pair of wires for each cell pair. Current versus voltage and power versus voltage characteristics for GNB cell pairs under worst-case-hot (WCH) end-of-life (EOL) conditions are shown in Figure 3 and Figure 4, respectively.

A blocking diode circuit for each cell pair prevents the battery from discharging through the solar cells during eclipse periods. In order to minimize power losses from this diode, an ideal diode circuit is used that simulates normal diode response through the switching of a MOSFET. This approach is suitable given that there are no high-speed switching requirements for these circuits. The ideal diode can operate with a voltage drop between 20 and 40 mV, significantly reducing power generation losses over a more conventional Schottky diode.

GNB uses two 5.3Ah lithium-ion batteries for energy storage, each with its own BCDR. Each battery consists of a single cell. Under nominal conditions, only one BCDR/battery is active on the bus, with the other held in reserve as a cold spare. Li-Ion batteries were chosen due to their much higher energy density compared to conventional Nickel-Metal-Hydride or Nickel-Cadmium batteries, and the particular Li-Ion cell used on GNB was selected based on its excellent charge and discharge performance over a wide temperature range.

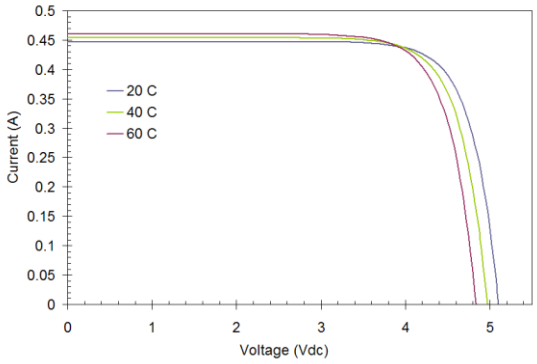

Figure 3: Current-Voltage Characteristics for GNB Solar Cell Pairs

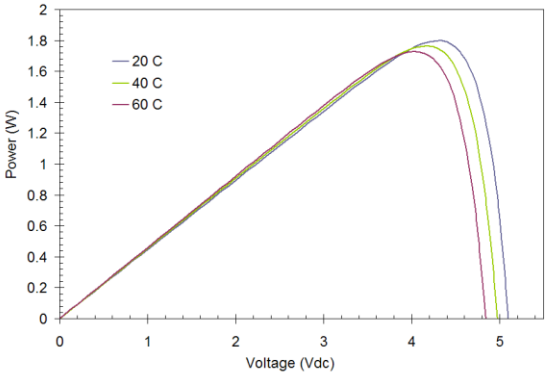

Figure 4: Power-Voltage Characteristics for GNB Solar Cell Pairs

System Topology

By conventional nomenclature, the GNB power system topology can be regarded as a direct energy transfer bus, in that its solar panels are connected directly to spacecraft loads without series regulation (Figure 2). However, this architecture can also be regarded as a peak power tracking system, since the operating BCDR regulates the bus and solar array voltage to a desired setpoint and can perform peak power tracking when required. GNB is rare in this hybrid DET/PPT topology, in that the bus is fully regulated by the operating BCDR against battery voltage variations, but with all solar array current not used for battery charging transferred directly to spacecraft loads. The BCDR controls the bus voltage to a fixed point of 4.4V by default, which corresponds to the average maximum power point of illuminated solar panels during each period of insolation. The BCDR can also be run in peak power tracking (PPT) mode, which varies the system voltage to maximize battery charge current. Batteries are charged using a constant-current/constant-voltage profile. When the battery reaches a full voltage of 4.1V, the BCDR

begins to raise the bus voltage towards array open circuit whilst maintaining the full cell voltage.

Topology Rationale

The rationale for selecting full parallel regulation was two-fold. First, the parallel-regulated option allows much greater solar power generation without impacting the efficiency of array-to-load power transfer. With the exception of subsystems on centrally-regulated power supplies, all load current flows directly from the solar array through the power board to point-of-load without conditioning, and thus, transport efficiency in the forward path is maximized. High power production and transfer efficiency are important for spacecraft running high-demand loads on a power-limited platform, which is the case for GNB. Second, a fully-regulated bus greatly increases the accuracy of spacecraft power analysis, since—in a regulated bus—the solar array operating voltage is deterministic, and spacecraft power generation can therefore be assessed without the need for an accurate model of battery voltage variations, which is difficult to develop and validate.

Full parallel regulation is made possible by the close matching of solar array and load input voltages. All spacecraft loads are designed to accept any voltage across the full solar panel range of operation, and thus, no series converters are needed to decouple the array from the bus. Instead, the BCDR simply converts its battery voltage to a desired operating point at the bus, with both the solar panels and the bus clamped at this setpoint. (It is instructive to view this system as a battery-regulated DET topology, but with a programmable battery output voltage enabled by the BCDR.)

Another noteworthy advantage of the GNB architecture is that, following launch vehicle separation, the solar panels cannot be disconnected from the bus by any means. Thus, in the event of a major battery or BCDR fault, the battery is designed to be automatically disconnected from the bus, allowing the spacecraft to be run as a ``sun-sat'', either permanently or until a second BCDR is brought on-line.

Simple Analysis

A simple analysis can be performed which demonstrates the superior efficiency of the GNB architecture over competing PPT bus designs. Consider the four canonical options for PPT, shown in Figures 5-8. Each of these systems are functionally equivalent to GNB, inasmuch as they each provide full solar array regulation as well as peak power tracking functionality.

We can compare these options using the simple method of Huynh and Cho [7]. Let r represent the fraction of a given orbit that a spacecraft is in eclipse, such that $r \leq 1$ and the sunlit period for the spacecraft is 1-r. Next, assume that every regulator in a given topology operates with the same constant efficiency $\eta \leq 1$ as well. Other inefficiencies such as harness, switch and battery losses are neglected.

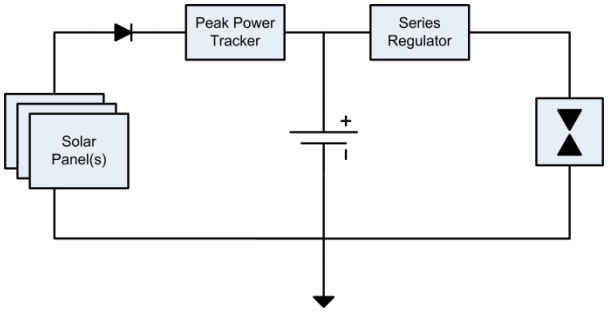

Figure 5: Series-Regulated PPT Topology

First, consider the series-regulated topology (Figure 5). During periods of sunlight, power delivered to the bus from spacecraft solar panels must pass through two series converters—the peak power tracker and the series regulator—and thus, a product of power transfer efficiency and orbit fraction in sunlight can be written as $\eta^2(1\text{-}r)$. During eclipse periods, power delivered to the bus from the battery can also be said to pass through two converters, since eclipse power must not only traverse the series regulator, but also must first have passed through the peak power tracker during sunlight in order to be stored in the battery. Thus, the eclipse efficiency – orbit fraction product is $\eta^2 r$. Summing these two fractions for the entire orbit, the efficiency of the series-regulated PPT system can be written as:

$$\frac{P}{P_0} = \eta^2(1-r) + \eta^2 r = \eta^2$$

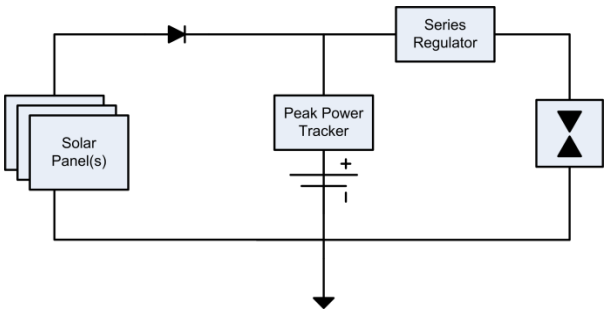

Figure 6: Parallel-Series PPT Topology

A similar argument can be applied to the parallel-series regulated PPT topology (Figure 6). During sunlight, load power passes through the series regulator with an efficiency – orbit fraction product $\eta(1\text{-}r)$. During eclipse, load power can be said to pass through the peak power tracker twice, since this power must first have entered the battery, and then passed through the series

regulator to the bus, giving an efficiency – orbit fraction product of $\eta^3 r$ and a complete orbit efficiency of:

$$\frac{P}{P_0} = \eta(1-r) + \eta^3 r$$

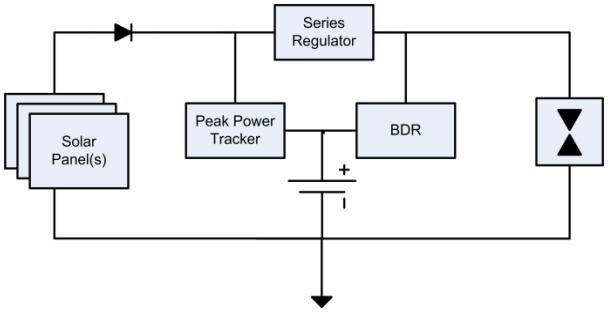

Figure 7: Series-Parallel PPT Topology

Huynh and Cho [7] use this method of analysis to propose the more efficient series-parallel bus shown in Figure 7. In this topology, sunlight power passes through a series regulator with efficiency product $\eta(1-r)$, and eclipse power passes through the peak power tracker in sunlight and the battery discharger in eclipse, yielding an eclipse product of $\eta^2 r$ and an orbit power efficiency of:

$$\frac{P}{P_0} = \eta(1-r) + \eta^2 r$$

The options presented in Figures 5-7 are all fully-regulated bus designs, in that their bus voltage can be completely decoupled from both the battery and solar array. A more common, more efficient bus (the battery-regulated PPT topology) is shown in Figure 9.

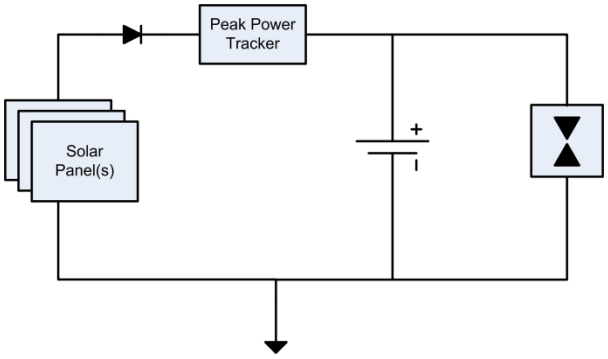

Figure 8: Battery PPT Topology

In the battery-regulated PPT topology, the array is decoupled from the bus, and the bus voltage follows the battery in both eclipse and sunlight. This topology will have all power pass through the series regulator, with an efficiency of:

$$\frac{P}{P_0} = \eta$$

which must always be more efficient than any of the fully-regulated bus designs considered previously.

We now compare these options to the GNB parallel-only regulated topology, which is equivalent to the series-parallel topology, but without the central series regulator. With reference to Figure 2, in the GNB system, load power in sunlight is passed directly from the arrays to the bus, giving unity efficiency. Power during eclipse will necessarily have traversed the BCDR twice before arriving at the loads, and will therefore have an eclipse efficiency product $\eta^2 r$, similar to the series and parallel-series topologies. Thus, the GNB orbit power efficiency can be written as:

$$\frac{P}{P_0} = (1-r) + \eta^2 r$$

which is greater than any other PPT option for practical values of r and η. The efficiency of the GNB architecture can be even further increased by having the BCDR connect the battery directly to the bus during eclipse, giving an orbit power efficiency of:

$$\frac{P}{P_0} = (1-r) + \eta r$$

The GNB system therefore achieves highest efficiency with the smallest number of switching converters than other PPT topologies, all things being equal.

It is not the case that parallel regulation has simply been overlooked in past spacecraft designs. Rather, it is more likely that few spacecraft have been able to match solar array and load voltage ranges closely enough that parallel regulation can be viewed as practical. (Indeed, in [6] Clarke identifies one of the greatest difficulties associated with parallel-only regulation as matching the array characteristics to the bus.) The GNB design is quite advantageous in this sense. Further, the benefits of parallel-only regulation suggest that it can be worthwhile to ensure close matching of solar arrays and loads early in a new spacecraft development program.

BATTERY CHARGE/DISCHARGE REGULATOR (BCDR) OVERVIEW

Pictured in Figure 9 and Figure 10, the GNB BCDR is responsible for both regulating spacecraft batteries as well as setting the system operating voltage as described above. The BCDR/battery combination consists of a small PCB affixed to a battery via two thermally insulating battery collars. The BCDR is highly modular and therefore can be easily integrated into pre-existing

designs. The BCDR speaks NanoSatellite Protocol (NSP) over SMBus by default, which can be changed to any two-wire bus and protocol as required. Multiple BCDRs can be operated in parallel at once, though this is not a baseline approach. Instead, the GNB architecture uses a single BCDR to regulate the bus, with the second unit kept offline as a spare.

Figure 9: GNB Battery Charge/Discharge Regulator (BCDR), Top

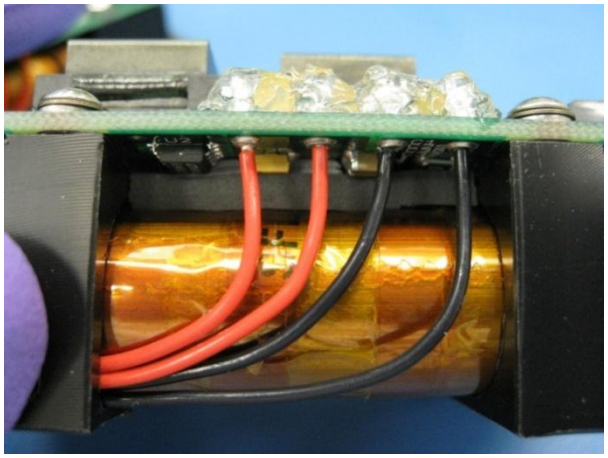

Figure 10: GNB BCDR, Side

Overview of Operation

The BCDR separates the main power bus from the battery using a two-port bi-directional split-Pi (boost-buck) converter, which regulates the bus voltage to either a fixed value (fixed mode) or a variable value to maximize battery charge current (PPT mode). Both modes allow the battery to charge as rapidly as possible up to a programmable limit.

The BCDR is driven by a microcontroller and is autonomous in its operation. The BCDR does not require any intervention to keep the spacecraft power system healthy. Nevertheless, more than 50 different BCDR parameters can be read on request by spacecraft computers, such that BCDR health and operation can be continually monitored if desired.

Once the BCDR is mated to its battery, the unit is always at least partially powered. A dedicated active low enable line is used to deactivate the BCDR processor, effectively turning the unit OFF and ensuring minimal loading of its battery. When connected to the spacecraft, each BCDR receives its enable line from the power board. This line is pulled low when the satellite is deactivated (i.e. when the satellite is on the launch vehicle) by spacecraft separation switches, and the default BCDR enable line is pulled high upon spacecraft deployment.

Figure 11 presents a simplified model of the BCDR power stage, which operates as either a buck or boost converter depending on which half-bridge is driven. The BCDR provides continuous current at both ports by virtue of its two ``outrigger'' inductors, contrary to the more conventional buck-boost topology.

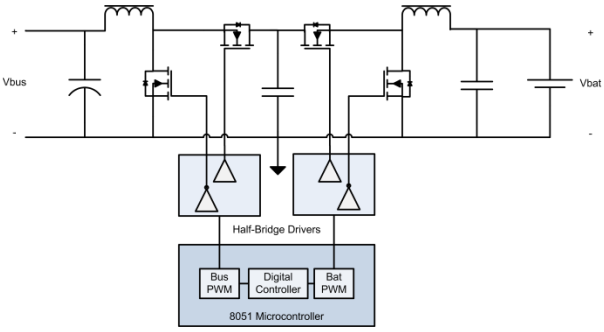

Figure 11: Simplified BCDR Topology

Both converter half-bridges are driven at approximately 100 kHz. In the nominal case, the duty cycle of one half-bridge is varied while the other has its high-side MOSFET ON at almost 100% duty cycle. Driving the battery-side half-bridge in Figure 11 with the high-side of the bus half-bridge held ON gives the canonical boost transfer function from the battery to the bus, in accordance with:

$$\frac{V_{bus}}{V_{bat}} = \frac{1}{1-D}$$

where D is the converter duty ratio. Conversely, the bus-side half-bridge can be PWM driven, with the high-side of the battery half-bridge held ON, giving a buck transfer function from the battery to the bus:

$$\frac{V_{bus}}{V_{bat}} = D$$

When the operating spacecraft battery is full, the BCDR supports a ``discharge only" mode of operation. This is useful in cases where small battery discharges are necessary for load-leveling, but where any further charging is undesirable. In this mode, a high-side diode on the battery bridge is used for discharge to the bus, providing a current-unidirectional characteristic to prevent unwanted battery charge current.

Digital Modulation and Control

The BCDR employs digital pulse-width modulation, which offers several advantages. Since the BCDR already requires a microcontroller to implement command and data handling functions, the same processor can be used for both telemetry gathering and control as well, reducing parts count and simplifying controller tuning and testing. Each BCDR half-bridge is driven by a dedicated 8-bit digital PWM bus, the duty cycle of which is calculated using a feedback control loop operating at 374 Hz.

An important point is that the worst-case transient performance of the BCDR cannot be worse than the transient response of the battery. That is to say, the worst-case response of the BCDR is to have its output voltage sag in proportion to the battery voltage by the regulator conversion ratio V_{bus}/V_{bat}. Nevertheless, the BCDR control loop is still sufficiently fast to provide relatively stiff output regulation.

Telemetry

Battery voltage, bus voltage, battery current and battery temperature are gathered using the microcontroller 12-bit ADC and software-defined filters. ADC telemetry is sampled at different points during converter switching, such that any switching noise aliases to DC [8].

Software

The onboard software is a critical component of the BCDR, and it was intended that on-orbit reprogramming of the base program not be allowed. However, software provisions are nevertheless made for uploading expansion code on-orbit. This is nominally intended to allow modifications of the peak power tracking algorithm, but can also be used to completely take control of the BCDR from the base program. The BCDR employs a rapid-access triple-voting error detection and correction (EDAC) file system, and performs periodic file system scrubs to correct and flag SEU-induced bit-flips.

POWER BOARD

The GNB design uses a central power distribution and switch board (power board, Figure 12). The power board interfaces the solar panels and BCDRs to the bus through a central main switch, and uses both latching (resettable) and non-latching (non-resettable) switches for spacecraft loads. On-board computers and the UHF receiver are connected to non-latching switches, which will briefly glitch on overcurrent but cannot be permanently turned OFF. The power board provides conditioned power at 3V, 5V, and either 3.3V (for GPS receivers used on AISSat-1 and CanX-4/-5) or 10V (for star trackers used on BRITE).

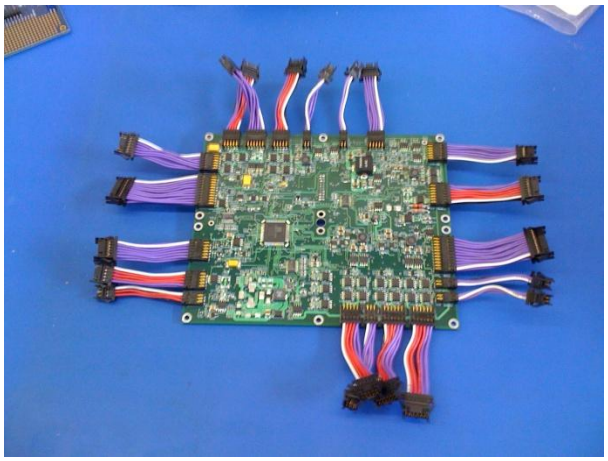

Figure 12: GNB Power Board

The power board uses three separate 12-bit ADCs for telemetry gathering, each of which has its own internal temperature sensor and 16 separate channels. A 12-bit digital-to-analog converter (DAC) is used to drive three programmable constant current sources for three 30 Ohm magnetorquers, each with a maximum current output of approximately 140 mA. The ADCs, DAC, and two on-board computers communicate with the central power controller FPGA using a dedicated Serial Peripheral Interface (SPI) bus.

The default power board design for GNB has 14 resettable and 3 non-resettable switches for spacecraft loads, each with a hardware-defined current limit. Spacecraft computers connect directly to the power board so that a reconfiguration can be performed to allow spacecraft operations using only a single OBC in the event of one computer failing on-orbit.

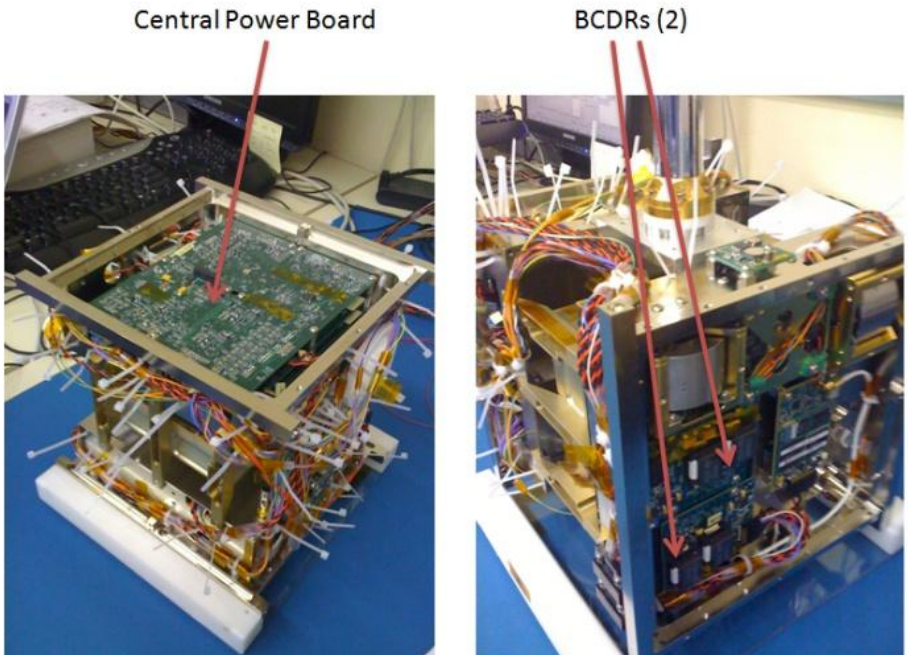

Figure 13: AISSat-1 Integrated Power System

INTEGRATED POWER SYSTEM

Figure 13 shows the fully integrated GNB power system for AISSat-1. At present, three complete GNB power systems (AISSat-1, UniBRITE and BRITE-Austria) have passed acceptance testing and have been delivered for their respective flight integrations.

PEAK POWER TRACKING ON GNB SPACECRAFT

Overview

The main problem associated with solar array peak power utilization is well-known and thoroughly discussed in the available literature. To briefly summarize the problem, we return to Figure 4, which depicts the power versus voltage curves for GNB solar cell pairs under hot, cold and nominal conditions. Figure 4 clearly illustrates that a maximum power point (MPP) exists in each case, and is a function of voltage and temperature. Hence, the problem of peak power tracking can be simply stated: find a way to automatically determine the voltage V_{mpp} at which maximum solar power is generated, at a given temperature and level of insolation [5]. While it is possible to have multiple local maxima under some conditions, it is generally the case that some overall power optimum will exist for a given array design [5].

While much literature exists that explores relatively exotic PPT methods, the majority of available work appears to focus on so-called perturb-and-observe algorithms. In the most general sense, P&O involves disturbing the quiescent operation of the solar array and analyzing the result, in order to gain insight into the maximum power point (MPP) location. The archetypal perturb-and-observe algorithm dithers the solar array voltage and employs both rapid telemetry gathering and logic to determine whether the MPP is at a higher or lower voltage than the initial setpoint. Once the MPP is found, an oscillation will generally occur about that point. Such oscillations can be reduced by decreasing the perturbation step-size, but this has the negative consequence of slowing the algorithm and increasing vulnerability to noise. Some methods have been developed which employ fuzzy logic control techniques to optimize the magnitude of each subsequent perturbation [5], though such techniques are beyond the scope of this work.

Peak Power Tracking using BCDRs

The GNB power system architecture was designed to enable peak power tracking. However, it was not until late into hardware development that options for implementing PPT using GNB BCDRs were investigated in earnest.

Initial Trades and Peak Current Tracking (PCT)

The process of evaluating and trading different PPT methods for GNB was first and foremost tempered by hardware capabilities. The BCDR, like all digital controllers, has finite bandwidth; finite telemetry sampling rates; finite precision; and a limited number of inputs that can be used for peak power tracking. In particular, a key telemetry point required by most PPT algorithms—solar array current—is not measured by the BCDR. Given the parallel-regulated nature of the GNB

architecture, knowledge of solar array current would require that the BCDR communicate with the power board, which would defeat the advantage of autonomous operation. While this may appear limiting, the absence of array current telemetry ultimately drove PPT development in a somewhat unconventional but beneficial direction.

It was decided early that the PPT algorithm would use a perturb and observe method as its baseline. This was chosen in the interest of reduced mathematical and computational complexity, and because a wealth of literature was available regarding such algorithms. Also, it was desired that the PPT algorithm be executed as an expansion module called directly from the main control loop, and then used to augment the base algorithm as opposed to taking complete control of the converter. This was in order to minimize required PPT functionality and reduce development time and risk. Thus, it was decided that PPT code should only act to change the BCDR bus voltage target, without altering any other software or hardware settings.

Finally, since the BCDR could not directly measure solar array power, it was decided that the PPT algorithm should instead attempt to maximize battery charge current. It was immediately realized that this approach—referred to here as *Peak Current Tracking* (PCT)—would provide important additional benefits over conventional PPT techniques. Specifically, an algorithm that attempts to maximize battery charge current would also act to minimize battery *discharge* current, which can dramatically increase battery life by ensuring minimal battery discharge under a given load demand profile. This has come to be viewed as a significant advantage over conventional PPT algorithms.

Dither Frequency

A low-frequency dither—well within the bandwidth of load regulators and below the response of reactive elements in the power system—is used for peak current tracking on GNB. The default algorithm dithers the bus at approximately 0.15 Hz, and can be easily changed operationally. The default dither frequency is inside the telemetry-gathering capabilities of the BCDR, allowing sufficient sampling of relevant telemetry during each PCT frame. Moreover, instead of requiring the algorithm to run at high frequency with respect to spacecraft subsystem activity, the low-frequency PCT instead operates very slowly relative to most load fluctuations. Such fluctuations add noise, but—provided they are not phase-locked with the PCT dither—do not introduce any DC error [8]. The disadvantage of low-frequency dithering is low bandwidth and poor transient performance. However, the lower-frequency approach is easily and robustly implemented, and its poor transient characteristics are offset by the fact that the PCT approach automatically compensates for BCDR efficiency and load variations [8].

PCT Algorithm Evaluation and Selection

The first Peak Current Tracking algorithm used an extremely simple perturb-and-observe algorithm, which would increase the solar array operating voltage in a given direction as long as battery charge current increased. This algorithm would start by increasing the bus voltage by a given voltage trim (step-size); wait for a specified settling time; then produce an error signal between the previous and measured battery current. A charge current increase would prompt another voltage increase, whereas charge current decrease would result in a voltage decrease. This algorithm, while simple and computationally inexpensive, was found to experience unavoidable oscillations about the maximum power point, and was furthermore easily confused by fluctuating load profiles.

A different and particularly interesting concept for BCDR PCT involved using a pseudo-random dither. In this approach, a pseudo-random bit sequence is generated using a linear feedback shift register and used to determine when the bus voltage is dithered high or low. The bitstream is clocked at a relatively low frequency. When the stream is at ‘1’, the bus voltage is increased by a pre-defined trim, and when the stream is at ‘0’, the voltage is decreased by the same step-size. Prior to each change, a measurement of battery current is made, and at the end of the bitstream, current measurements corresponding to high and low bits are averaged and their deviation from the mean evaluated. These deviations, in turn, are used to examine which voltage setpoint resulted in a net battery current increase, with the search direction of the algorithm moved to a higher or lower voltage accordingly.

This concept was compelling but ultimately complex to implement. First, it was found that test algorithms had to be run at very low frequency in order to obtain valid battery current measurements at each setpoint, since the process of controlling the bus to a new voltage inevitably requires settling time prior to measurement. Consequently, the frequency of the bitstream had to be reduced significantly, resulting in slow convergence. Second, test algorithms were difficult to implement within the memory-limited BCDR expansion code framework. While pseudo-random techniques are known to be extremely powerful, initial testing indicated that a somewhat simpler and less expensive algorithm may yield equally good resolution on the optimal system operating point.

The final PCT algorithm developed for the BCDR was a variant of the relatively straightforward P&O gradient method, but with the incorporation of a simple voltage settling criterion as well as optional low-frequency external supervision. This approach, referred to here as a three-point gradient method, involves dithering the bus voltage high and low, and then evaluating battery current changes between voltage setpoints as in previous sections. However, whereas most P&O algorithms only examine two setpoints (high and low), the three-point algorithm also uses the nominal (intermediate) voltage as a reference, permitting evaluation of actual charge current *gradients* across the range of test values. In this approach, the setpoint is changed in the direction of increasing charge current only when a clear gradient is found across all three test voltages. Then, if such a gradient is found, the voltage setpoint is nudged in the appropriate direction. In other words, if an increasing current gradient is measured across the low-mid-high range, the bus voltage is increased; if an increasing current is measured across the high-mid-low range, the bus voltage is decreased; and if no clear gradient is detected, the bus voltage is unchanged. This algorithm is both robust against load power transients and is also able to track and settle on a maximum charge point with little oscillation. Evaluation of the nominal setpoint is the key to achieving this performance: only voltage excursions that result in a clear and measurable gradient across the base setpoint are used to adjust it. Otherwise, the nominal voltage is maintained until a gradient is found, resulting in much greater dwell times at optimal setpoints than could otherwise be achieved.

PCT Overview

Figure 14 and Figure 15 present a detailed overview of the three-point gradient PCT algorithm. The algorithm involves three voltage test cases—nominal, high, and low—which are separated by programmable settling times and dwell times at the nominal setpoint. The algorithm makes brief excursions to the high and low test voltages and records battery telemetry, but otherwise remains at the nominal setpoint for as long as possible, since it is assumed that, in steady-state, the nominal voltage will correspond to the desired operating point.

The PCT algorithm is bounded by maximum and minimum allowable voltage setpoints, corresponding to MPP extrema expected by spacecraft thermal analysis.

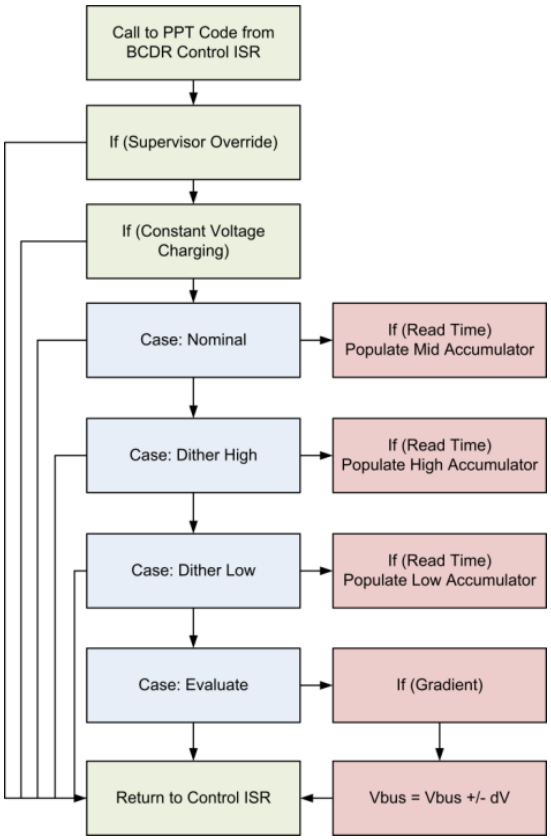

Figure 15: PCT Algorithm Flowchart

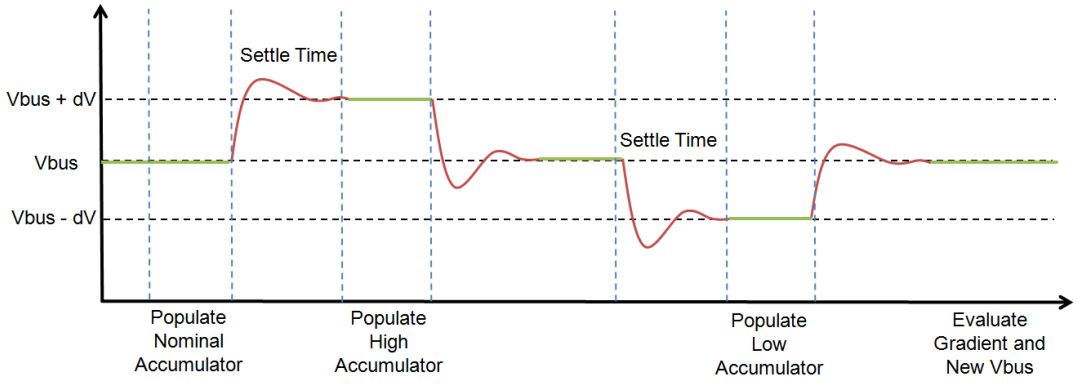

Figure 14: PCT Algorithm Sequence

The default run-time of the entire algorithm is approximately 1s total. Each aspect of the algorithm—total runtime, number of accumulator readings, and settling time—are parameterized as BCDR files, and can be changed by spacecraft operators without needing to upload new code. As well, the number of times the algorithm remains at a given setpoint—referred to as its "sit count"—is stored in a dedicated file, and can be logged over time to assess how well the algorithm loiters at a favorable operating point.

Low-Speed Supervisor

In addition to the gradient-based peak power tracking algorithm, a level of low-speed control supervision can be added using solar panel temperature correlation. When active, this supervisory algorithm nominally runs from one of the two GNB on-board computers as part of the spacecraft housekeeping thread. At a predetermined rate (0.0167 Hz by default), the supervisor measures the temperatures of all six solar panels, and takes the warmest value as an indicator of the most illuminated one. An estimate of the panel's maximum power point is then made, and—if the supervisor determines the BCDR to be more than a certain percentage off the calculated value—can override the PCT algorithm and command the BCDR to what it believes to be the correct setpoint. The supervisor does not operate during eclipse.

While it is not necessarily the case that the primary algorithm will identify the solar panel MPP as the best operating point for battery charging, analysis and testing have indicated that, practically, the closed-loop controller will almost always land in the MPP vicinity. This is because all primary GNB subsystems are constant-power loads, and thus, a departure from the array MPP will either increase load current consumption or move the array towards open-circuit, both of which decrease available charge current. Nevertheless, if the supervisor is observed to pull the BCDR off its desired setpoint too often during operations, it can either be turned OFF or its MPP error bounds changed. Furthermore, as a completely different alternative, the comparatively noisy BCDR closed-loop algorithm can be abandoned, and the spacecraft run using only the low-speed temperature-correlated peak power tracker.

PERFORMANCE EVALUATION

The three-point gradient PCT method has, at the time of this writing, been extensively tested and refined in its standalone mode, and has also been tested using periodic supervisor action.

Resistive Load Testing

Initial PCT tests were performed using a set of programmable resistive loads (e-loads) in parallel with the BCDR and a solar array simulator (SAS). As expected, regardless of whether the solar array simulator is active, running the algorithm under resistive loading causes the

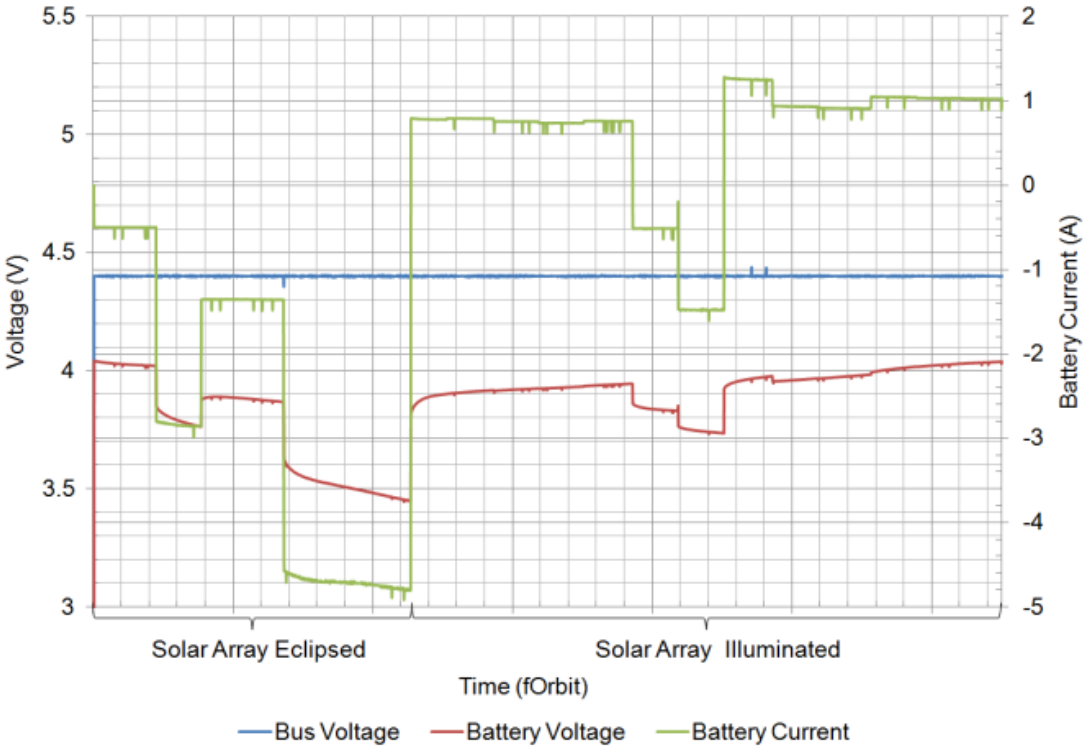

Figure 16: Orbit Simulation with Fixed-Mode BCDR

BCDR to immediately drive the bus voltage to its lower bound. This is not surprising: because resistive loads have a constant, linear IV slope, decreasing voltage across the load will always decrease current consumption. With the solar array simulator ON, the PCT drops the bus voltage to maximize battery current, since array current output is relatively constant in the range $0<V_{sa}<V_{mpp}$. With the solar array simulator OFF, the PCT still drops the bus voltage, this time to minimize battery discharge to the load.

In all resistive load cases, the PCT converges to its voltage floor within seconds. This illustrates a key difference between the PCT algorithm and a canonical PPT method: in the latter case, attempting to maximize array power would not result in maximum battery charge current at all, since the array MPP would not correspond to the point of minimum load current draw. Indeed, if the linear load were equal to the array MPP impedance V_{mpp}/I_{mpp}, then maximizing solar array power would not generate any battery charge current at all! As the primary objective of spacecraft PPT is to charge the battery as rapidly as possible, this is viewed as a disadvantage of the conventional approach.

Constant Power Loads and Orbit Simulations

Of course, the purely resistive loading scenario is not a realistic one. Since spacecraft loads are constant power in nature, a series of constant power load tests were performed with the same SAS/programmable load setup as before. In initial tests, the programmable load was put into constant power mode, and the solar array simulator commanded to varying I-V characteristics. The initial test method was to override the PPT algorithm using the low-speed supervisor, commanding the BCDR to an operating point far from the array MPP. Then, the override condition would be removed. It was found that the BCDR was always able to converge to a maximum current point without fail, regardless of its initial value. In the case of light constant power loading, the PPT algorithm would tend to settle at a voltage slightly below the maximum power point of the array, where it was able to extract slighly more battery charge current than at the MPP. This situation becomes pronounced when the constant-current region of the solar array is given steeper slope. Depending on load power demand, a small decrease in array voltage gives a marked increase in charge current under such circumstances, which the algorithm is able to track.

Ultimately, complete spacecraft simulations were undertaken using the array simulator and programmable load, with scripts written to vary both power demand and solar array characteristics in an operationally representative way. Table 1 presents the varying I-V profile used in the solar array simulator for each orbit during these trials, as well as the time-varying constant power load profile. Of particular note is the presence of high-frequency load activity during periods of insolation. This corresponds to anticipated GNB sun sensor activi-

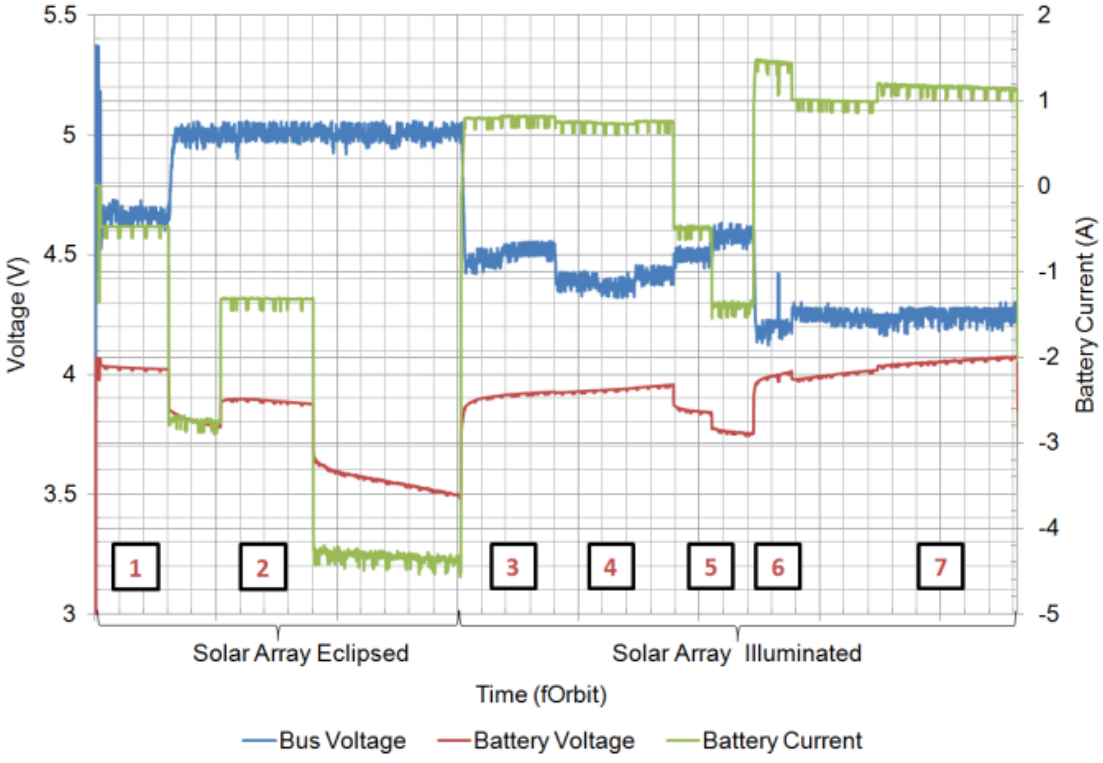

Figure 17: Orbit Simulation with PCT-Mode BCDR

ty, with multiple sensors being turned ON and OFF at approximately 1 Hz in sunlight. Simulating this fluctuation was important in order to ascertain how well the PPT can function through spacecraft noise.

Table 1: Summary of Solar Array and Load Profiles used in BCDR Orbit Simulations

Duration (s)	State	V_{oc} (V)	V_{mpp} (V)	I_{sc} (A)	I_{mpp} (A)	Load (W)
420	OFF	0	0	1.837	0	4.4
840	OFF	0	0	1.839	0	8.6
840	OFF	0	0	1.841	0	14
240	ON	5.8	5.139	1.842	1.75	3 + 0.45 @ 1Hz
300	ON	5.8	5.195	1.843	1.75	3 + 0.45 @ 1Hz
300	ON	5.7	5.054	1.845	1.75	3 + 0.45 @ 1Hz
300	ON	5.7	5.018	2.109	2	3 + 0.45 @ 1Hz
300	ON	5.7	5.084	2.11	2	8.6 + 0.45 @ 1Hz
300	ON	5.7	4.955	1.587	1.5	14 + 0.45 @ 1Hz
300	ON	5.7	4.929	1.587	1.5	4.9 + 0.45 @ 1Hz
300	ON	5.7	4.906	1.848	1.75	4.9 + 0.45 @ 1Hz
300	ON	5.7	4.888	1.849	1.75	4.9 + 0.45 @ 1Hz
300	ON	5.7	4.872	1.837	1.75	4.9 + 0.45 @ 1Hz
300	ON	5.7	4.861	1.82	1.575	4.9 + 0.45 @ 1Hz
300	ON	5.7	4.853	1.781	1.4175	4.9 + 0.45 @ 1Hz

Initial orbit simulations were performed using the BCDR in its default fixed state for benchmarking purposes. In this state, the BCDR controlled the solar array operating point to 4.4V. Figure 16 illustrates bus voltage, battery voltage, and battery current during a single orbit using the fixed BCDR mode and the solar array/load profiles from Table 1.

Next, the BCDR was commanded into PPT mode and run through the same orbit simulations. Figure 17 presents the results from this trial run.

Figure 17 illustrates several important features of PPT operation, which are enumerated below corresponding to the numbered sections of the graph.

- **Light load during eclipse**. Battery discharge current is small, and the PCT algorithm converges to an average bus voltage of approximately 4.55V, which minimizes battery discharge current.
- **Heavy load during eclipse.** Battery discharge current is large, varying from approximately 1.2A to 4.5A. The PCT algorithm drives the bus setpoint to its voltage ceiling of +5V in order to minimize battery discharge. Under heavy discharge, higher constant power load voltages reduce current, Ohmic losses and converter inefficiencies.
- **Medium load during sunlight.** The algorithm actively tracks the solar array maximum power point, which increases slightly during (3) from approximately 5.14V to 5.2V. With the addition of an approximately 0.7V jump from the bus to the SAS across a blocking diode, it was observed that the PCT algorithm closely follows the array MPP.
- **Medium load during sunlight**. The algorithm follows the solar array MPP as it drops to roughly 5.02V and then increases slightly to 5.1V.
- **Heavy load during sunlight**. The battery discharges to provide load-leveling, and the PCT algorithm increases the bus voltage to achieve solar array PPT tracking. This is necessary due to long harness length between the SAS and programmable load, which gives rise to increased Ohmic losses and voltage drop under high load.
- **Light load during sunlight**. The BCDR moves to an operating point slightly below the solar array MPP to maximize battery charge current.
- **Medium load during sunlight**. The PCT algorithm again actively tracks the solar array MPP with accuracy.

These tests illustrate the advantages of the BCDR PPT algorithm. Of particular note is the second case in Figure 17, in which the BCDR drives the bus voltage to it ceiling to reduce discharge current. It is well-known that higher voltages will generally give higher efficiencies at higher power—what is important to observe here is that the BCDR goes to the higher voltage operating point *without being told this rule*. This emergent behavior of the PCT algorithm is important and further illustrates its advantages.

Table 2 provides a summary of results from the fixed and PCT orbit simulations, in terms of battery figures-of-merit. It can be seen that operating the BCDR in its PCT mode offers clear advantages over fixed mode in terms of battery discharge levels, which in turn increases battery longevity. In general, the PCT mode provides faster battery charging as well as battery discharge management, offering two key advantages for battery health and performance.

Table 2: Comparison of Fixed and PCT Modes during Orbit Simulations

Telemetry	Default	PPT	% Difference	Advantage / Comment
Avg I_{bat} (A)	-0.758	-0.616	18.68%	CCT: Reduced Battery Discharge
Avg V_{bat} (V)	3.852	3.880	0.72%	Marginal Change
Avg V_{bus} (V)	4.400	4.576	3.99%	CCT: Higher V_{bus} reduces losses
Max I_{chg} (A)	1.284	1.485	15.65%	CCT: Faster Battery Charge
Max I_{dischg} (A)	4.920	4.574	7.03%	CCT: Reduced Battery Discharge
Max *DOD* (%C)	39.67%	32.72%	17.52%	CCT: Shallow Cycling / Increased Life

FUTURE WORK

The PCT approach is shown to be a unique and beneficial means of managing spacecraft batteries. However, even the 3-point gradient method presented in this paper is susceptible to discontinuities in the power curve; and a discontinuity that maximizes battery charge or

minimizes battery discharge may not be recognized by the PCT algorithm described herein.

One possible discontinuity is the case where the BCDR operates in a pass-through mode, connecting the battery directly to the bus. A gradient-based P&O algorithm would not necessarily recognize this mode of operation as globally efficient. Furthermore, PCT testing to date has not examined this case, given that bus-at-battery voltages are generally beneath the lower voltage threshold of the baseline PCT algorithm. The pass-through case will be investigated presently with actual spacecraft loads, which are important for an accurate evaluation. Should it be found that direct battery-to-bus connection is most efficient, augmenting the PCT algorithm to either periodically check this case or default to it during operations is expected to be straightforward.

CONCLUSIONS

This paper has described the design, analysis and implementation of an advanced high-performance power system for the SFL generic nanosatellite bus. The GNB power system uses an unconventional parallel-regulated topology with peak power tracking capabilities, which has been shown to be the architecture of greatest efficiency when solar array and load characteristics are closely matched. As well, a unique variation on peak power tracking, referred to here as Peak Current Tracking, has been shown to significantly reduce battery discharge levels and increase spacecraft power margins, and has furthermore been demonstrated in testing to be immune to high-frequency spacecraft load activity.

Several GNB missions are presently being developed, as its small design has proven quite capable of enabling ambitious missions at low cost. As well, the GNB power system has directly informed other design activities for larger spacecraft in turn. The benefits of microspace permeate, and spacecraft designs such as the SFL generic nanosatellite bus are at the forefront of innovation in satellite design.

ACKNOWLEDGEMENTS

The authors would like to thank both Nathan Orr and Mihail Barbu for their contributions to GNB power system development. As well, we would like to thank our customers, including:

- U. Vienna
- Defence Research and Development Ottawa
- Canadian Space Agency (CSA)
- Natural Sciences and Engineering Research Council of Canada (NSERC)
- MDA Space Missions
- Ontario Centres of Excellence (OCE)
- Norwegian Defence Research Establishment (FFI)
- Com Dev International

Additionally, we would like to thank our sponsors for their continued support, who include: AeroAntenna Technology Inc.; Agilent Technologies; Altera; Alstom; Altium; Analytical Graphics Inc.; Ansoft; ARC International; ATI; Autodesk; @lliance Technologies; Cadence; CMC Electronics; EDS; E. Jordan Brookes; Emcore; Encad; Honeywell; Micrografx; National Instruments; Natural Resources Canada; NovAtel Inc.; Raymond EMC; Rogers Corporation; Stanford University; Texas Instruments; The MathWorks; Wind River. Thank you all.

REFERENCES

[1] G. Bonin, *Small Satellite Capabilities in Canada: Review and Points of Interest*, Defence Research and Development Canada Report No. 15EA06, 2008.

[2] P. Stibrany and K. Carroll, "The Microsat Way in Canada", 11th CASI Astronautics Conference, Nov. 2000.

[3] A. Philip, *Attitude Sensing, Actuation, and Control of the BRITE and CanX-4/-5 Satellites*, Master's Thesis, 2008.

[4] G. de Carufel, *Assembly, Integration and Thermal Testing of the Generic Nanosatellite Bus*, Master's Thesis, 2009.

[5] T. Esram and P. Chapman, "Comparison of Photovoltaic Peak Power Tracking Techniques", IEEE Transactions on Energy Conversion, pp. 439-449, June 2007.

[6] C. Clark and A. Mazarias, "Power System Challenges for Small Spacecraft", European Small Satellite Services Symposium, 2006.

[7] P. T. Huynh, and B. H. Cho, " Design and Analysis of a Regulated Peak Power Tracking System", IEEE Transactions on Aerospace and Electronic Systems, No. 1, 1999.

[8] G. Bonin, *Power System Design and Analysis Tools and Power Electronics Implementation on Generic Nanosatellite Bus Spacecraft*, Master's Thesis, 2009.